The electrochemical stability of thiols on gold surfaces

R.C. Salvarezza, P. Carro

PII: S1572-6657(17)30754-3
DOI: doi:10.1016/j.jelechem.2017.10.046
Reference: JEAC 3606

To appear in: *Journal of Electroanalytical Chemistry*

Received date: 22 May 2017
Revised date: 17 October 2017
Accepted date: 19 October 2017

Please cite this article as: R.C. Salvarezza, P. Carro , The electrochemical stability of thiols on gold surfaces. The address for the corresponding author was captured as affiliation for all authors. Please check if appropriate. Jeac(2017), doi:10.1016/j.jelechem.2017.10.046

The electrochemical stability of thiols on gold surfaces

R.C. Salvarezza[+] and P. Carro*

[+]*Instituto de Investigaciones Fisicoquímicas Teóricas y Aplicadas (INIFTA), Facultad de Ciencias Exactas, Universidad Nacional de La Plata - CONICET- Sucursal 4 Casilla de Correo 16, (1900) La Plata, Argentina.*

***Área de Química Física, Departamento de Química, Facultad de Ciencias, Universidad de La Laguna, Instituto de Materiales y Nanotecnología, Avda. Francisco Sánchez, s/n 38071- La Laguna, Tenerife, Spain*

Abstract

In this paper we present a comparative analysis of the electrochemical stability of alkanethiols, aromatic and heterocyclic thiols on the Au(111) and Au(100) faces in relation to the theoretical energetic data. The peak potential and surface coverage are used as the key parameters to estimate the electrochemical stability while work function changes, adsorption energies and surface free energies calculated from periodic DFT, including van der Waals interactions, are used for the theoretical estimation. We find that the peak potentials do not correlate with work function changes and adsorption energies in particular for aromatic and heterocyclic thiols. In contrast, the reductive desorption potentials for the different thiols show a good correlation with the surface free energy of the SAMs estimated by density functional theory calculations. Surface coverage is a key factor that controls reductive desorption through van der Waals interactions.

Corresponding author:
Pilar Carro
Email: pcarro@ull.es

Introduction

The electrochemical behavior of self-assembled monolayers (SAMs) of thiols (RS) on gold and silver has been widely studied because it provides valuable information about their blocking ability for electron transfer, stability potential range and surface coverage (θ). In particular the main cathodic peak related to the reductive desorption in aqueous electrolytes that appears on a potential linear scan from the open circuit potential to the hydrogen evolution reaction potential region exhibits a peak potential (E_p) and a charge density (q) that have been widely used to estimate SAM stability and θ, respectively (Figure 1)[1-6]. This information is crucial in different applications of thiol SAMs on gold in aqueous solutions, such as sensor and biosensors [7], biomimetic systems [8], molecular coatings for nano/microfabrication [9] , and building blocks in complex catalytic surfaces [10] .

It is widely accepted that the thiol (RS) desorption process from a metal (Me) surface can be represented by the reaction

$$RS\text{-}Me + solvent + e^- = RS^-_{solv} + Me_{solv} \quad [1]$$

where $RS^-_{solv} + Me_{solv}$ stand for the solvated thiolates and metal surface [11]. Experimental data for Au(111) reveal that E_p depends on thiol concentration, and it is shifted negatively by 0.057 V/decade when the thiol concentration is increased, confirming that the desorption is a one-electron process [12]. Note that reaction (1) is a solvent substitution reaction, which results in a significant change in the electrode capacitance, and a significant change in the potential of zero total charge [13-15]. This fact induced errors in the estimation of θ from q values due to the failure to account for the double-layer charging contribution.

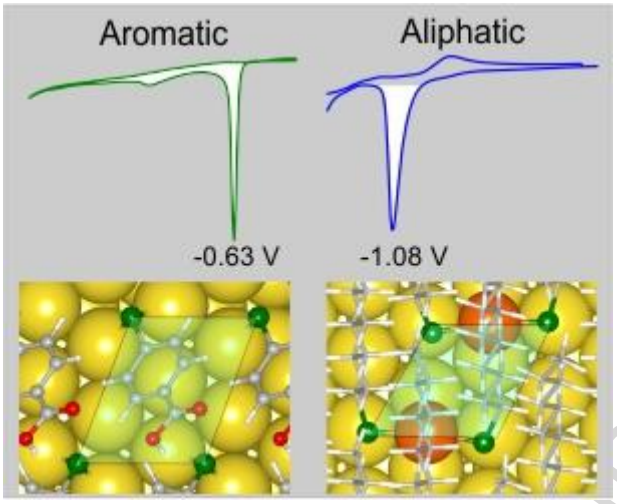

Figure 1. Upper: Typical reductive desorption voltammograms for aromatic (4MBA)[16] and aliphatic (C11) [16] thiols on Au(111). The peak potential value (E_p) and the charge involved in the peaks (white areas) are indicated. Lower: representation of the models used for DFT calculations: adsorbed thiyls for aromatic and staples moieties for aliphatic thiols. Golden: Au surface atoms, orange: Au adatoms, green: S atoms, gray: C atoms, white: H atoms, red: O atom.

Experimental data reveal that E_p is independent of the pH for values > 5 [17, 18] but moves slightly in the positive direction as the scan rate decreases from 0.05 to 0.005 V s^{-1} [19] indicating that reductive desorption is kinetically controlled. It has also been shown that E_p values also depend on the solvent [11], and the nature of the cations present in the electrolyte [6]. Therefore, a minimal requirement in using E_p as a criterion for SAM stability is that it is compared in identical experimental conditions.

The shape of the current-time transients corresponding to the reductive desorption in aqueous alkaline solutions is consistent with a nucleation and growth process of "holes" inside the thiol adsorbed layer [19-21]. This process should involve different contributions such as the thiol adsorption energy, which contains both the RS-Me bond strength and van der Waals interactions (vdW), and the hydration energies of the desorbed RS^- species and of the metal surface [22].

The importance of the S-Au bond strength has been clearly demonstrated as E_p becomes more negative for the same thiol SAM prepared on the open (100) [23] and Au(110) faces [17, 24],

where this bond is stronger, than on the compact Au(111) face [25]. On the other hand, the role of van der Waals (vdW) forces has also been revealed by the behavior of alkanethiol SAMs on the Au(111) face. In fact, linear E_p vs *n* (the number of C atoms) plots for $n < 12$ and pH values > 5 [1, 26] have been found for these thiols with a slope ≈ 0.03 eV/C atom (3 kJ mol^{-1}/C unit), [6] a figure somewhat lower to that expected for vdW interactions in hydrocarbon chains 0.08 eV [27, 28] due to the solvent effect in equation (1) [28]. This slope has been obtained irrespective of the scan rate used for E_p estimation [19]. The linear behavior in the E_p vs *n* plot for alkanethiols on the Au(111) surface is not surprising as the strength of the S-Au bond on the same crystalline face should not change very much with the hydrocarbon chain length and alkanethiols reach the same θ value (θ= 0.33) on this face, as revealed by STM images [4] and q after double layer correction [17]. Also, other energetic contributions such as desorbed thiolate-solvent, and solvent-metal interactions (equation (1)) are similar since alkanethiols are poorly soluble or insoluble in aqueous solutions and the hydration energy of the Au(111) surface is a constant. Note, however, that the hydrocarbon chain dependent shift was also attributed to the decreased ionic permeability in SAMs of longer alkanethiols [6].

The simple behavior observed for the reductive desorption of alkanethiol SAMs becomes more complex when aromatic or heterocyclic thiols are included in the same analysis since they have different S-Au bond strength [29], intermolecular forces dominated by π-π interactions, different surface coverage, and accordingly different surface structures [30]. In general they exhibit more positive E_p values than those found for alkanethiol SAMs, a fact that has been associated with the aryl group that withdraws electrons from the Au surface easier than the aliphatic chains, thus favoring reductive desorption [31].

Today, scanning tunneling microscopy (STM) and density functional theory (DFT) calculations have provided a great amount of valuable experimental and theoretical

information about surface structures, adsorption energies, and surface free energies for a large number of thiols on Au(111), and to a lesser extent on the Au(100) face [32]. Thus, it is now accepted that aliphatic SAMs on Au(111) for $n < 12$ are formed by RS-Au_{ad}-SR complexes, known as staples, at low and medium surface coverage [33]. Dense (3x4) ($n< 3$) or c(4x2) ($3<n<12$) [34] lattices ($\theta = 0.33$) formed by staple units have been observed on the Au(111) surface. On the other hand, it is not clear that this is the case for aromatic thiols [35] or heterocyclic thiols [34] on the same face Also, today there is no experimental evidence of staples for all kinds of thiols on the Au(100) face [30]. Therefore, it is timely to revisit the interpretation of peak potentials and electrochemical stability in the light of this information. In this work we correlate experimental E_p values reported in the literature for a large number of thiols with theoretical information obtained in our laboratory by using a functional including vdW interactions in order to understand the factors that control electrochemical stability of thiols on gold surfaces better.

Methodology

E_p values were taken from previous works. All of them were measured from reductive desorption peaks in alkaline solutions with Na^+ and K^+ cations at nearly pH 13 and v in the 0.02 /0.05 V s^{-1} which yields the same slope in the Ep vs *n* plots as much slower v values [19]. The surface structure of each thiol corresponds to the latest information which has been reported from STM images. The corresponding references are included in Table 1. The nomenclature employed in this paper was C_n for alkanethiols, where *n* denotes de number of carbon atoms with *n*=1,2,3,4,5,6,8 and 11, 2MBA: 2-mercaptobenzoic acid, 4MBA: 4-mercaptobenzoic acid, 4MPy: 4-mercaptopyridine, BZ: benzenethiol, and 6MP: 6-mercaptopurine

Computational Methods

We have performed new DFT calculations for different thiols or taken previous data from our Laboratory, all of them using the same functional including van der Waals interactions. In all cases we have modeling surface structures already described by STM formed by staples for alkanethiols and by thiyl radicals for aromatic thiols, unless otherwise ~~is~~ indicated in the text. Density functional calculations have been performed with the periodic plane-wave basis set code VASP 5.2.12. [36, 37] We have followed the scheme of non-local functional proposed by Dion et al.[38], vdW-DF, and the optimized Becke88 exchange functional optB88-vdW [39] to take into account van der Waals (vdW) interactions. The projector augmented plane wave (PAW) method has been used to represent the atomic cores [40] with PBE potential. The electronic wave functions were expanded in a plane-wave basis set with a 420 eV cutoff energy. Optimal grids of Monkhorst-Pack [41] with different k-point meshes have been used for numerical integration in the reciprocal space. The Au(100)-(1x1) and Au(111) substrates were represented by a five atomic layer and a vacuum of ~17 Å that separates two successive slabs. Surface relaxation is allowed in the three uppermost Au layers of the slab. The atomic coordinates of the adsorbed species were allowed to relax without further constraints. The atomic positions were relaxed until the force on the unconstrained atoms was less than 0.03 eV $Å^{-1}$. The adsorbates are placed just on one side of the slab and all calculations include a dipole correction. Radical species were optimized in an asymmetric box of sufficient size to avoid lateral interactions. The calculated Au lattice constant is 4.16 Å, which compares reasonably well with the experimental value (4.078 Å).[42]

The average binding energy per adsorbed thiol (RS) species on Au surfaces, E_b, is defined in Eq. [2]:

$$E_b = \frac{1}{N_{RS}}\left[E^{RS/Au} - E^{Au} - N_{RS}E^{RS}\right] \qquad [2]$$

where, $E^{RS/Au}$, E^{Au} and E^{RS} stand for the total energy of the adsorbate-substrate system, the total energy of the Au slab, and the energy of the RS radical, respectively, whereas N_{RS} is the number of RS radicals in the surface unit cell. A negative number indicates that adsorption is exothermic with respect to the separate clean surface and RS radical.

On the other hand, the reconstructed energy, $E_{rec,}$ to form the staples is defined by,

$$E_{rec} = \frac{E_{Au}^{R} - E_{Au}^{U} - n_{ad}E_{bulk}^{Au}}{N_{RS}} \quad [3]$$

where E_{Au}^{R}, E_{Au}^{U} correspond to the energy of reconstructed Au surface and unreconstructed Au surface per cell unit respectively; E_{bulk}^{Au} is the total energy of a bulk Au atom and n_{ad} is the number of Au adatoms in the surface unit cell. This energy is related to the Au adatom formation, which yields the RS-Au_{ad}-SR moieties. The E_{rec} value has been calculated for all alkanethiols from equation [4], its value being between ≈ +0.51 eV.

Therefore we define

$$E_b^* = E_b + E_{rec} \quad [4]$$

On the other hand, the Gibbs free energy of adsorption of each surface structure (γ) can be approximated through the total energy from DFT calculations by using equation [5]:

$$\gamma = \frac{N_{RS}}{A}(E_b^*) \quad [5]$$

where A is the unit cell area. Keep in mind that $\frac{N_{RS}}{A}$ represents de molecular density that is proportional to coverage, θ.

We have also evaluated the two contributions to E_b^*, namely the molecule-molecule (ΔE_{m-m}) and the molecule-Au substrate (ΔE_{m-Au}) as,

$$\Delta E_{m-m} = \frac{1}{N_{RS}}[E^{SAM} - E^{RS}] \quad [6]$$

$$\Delta E_{m-Au} = E_b^* - \Delta E_{m-m} \quad [7]$$

The change in the work function, ΔW, caused by SAM formation with respect to the clean Au(100) surface is defined as

$$\Delta W = W_{SAM} - W_{clean\_metal} \qquad [8]$$

Changes in the vertical component of the surface dipole due to the adsorption of the SAM, $\Delta\mu_{\perp}$,[43] are related to ΔW values by

$$\Delta W = \frac{-N\Delta\mu_{\perp}\, e}{\varepsilon_0} \qquad [9]$$

where *N* represents the molecular density of the SAM, e the elementary charge and ε_0 the permittivity of vacuum. The change in the surface dipole $\Delta\mu_{\perp}$ involves two components. The first component is μ_{SAM}, the molecular dipole moment of the SAM along the normal direction that represents the dipole moment along the surface normal of adsorbates embedded in a free-standing SAM (without the substrate). The second one is μ_{CHEM}, the change in the surface dipole resulting from the charge transfer between the adsorbate and the gold surface. We have calculated μ_{SAM} by using

$$\mu_{SAM} = \frac{[V_{SAM}(+\infty) - V_{SAM}(-\infty)]\epsilon_0}{e\,N} \qquad [10]$$

where $V_{SAM}(\infty)$ and $V_{SAM}(-\infty)$ are the asymptotic electrostatic potential on both sides of the SAM. Thus, μ_{CHEM} can be obtained from $\Delta\mu_{\perp}$ and μ_{SAM} values.

Results and discussion

Reductive desorption potentials (E_p), surface coverages (θ), and thiol lattices determined from experiments, and energetic parameters (E_b^*, γ), and work function changes (ΔW) estimated from DFT calculations for different aliphatic, aromatic and heterocyclic thiols on Au(111) are shown in Table 1. Data for some thiols on the Au(100) are also included.

In order to obtain a better comparison for the desorption data from the different crystal faces we need to refer E_p values to the corresponding potentials of zero charge (E_{pzc}). Values of E_{pzc} = 0.23 V and E_{pzc} = 0.08 V (vs SCE) in $HClO_4$ have been reported for the (111)-(1×1) and (100)-(1×1), respectively [44]. A similar value, E_{pzc} = 0.27 V (vs SCE), for the Au(111) surface has also been measured in $KClO_4$ [14]. This is an imporatnt point since differences in E_{pzc} explain the behavior for the reduction of cations on these gold surfaces [45]. Therefore, hereinafter we will use (E_p-E_{pzc}) with E_{pzc} = 0.23 V for Au(111)-(1×1) and E_{pzc} = 0.08 V for the Au(100)-(1×1) to cancel this effect. We have assumed that these E_{pzc} values are not significatively modified in alkaline solutions since desorption takes place in the double layer potential region where OH^- adsorption should be negligible. In fact it has been reported that at E < -0.5 V, the potential range of E_p shown in Table 1, the OH^- is totally desorbed from the Au(111) electrode surface [46].

The E_{pzc} is also important to understand the reductive desorption of thiols from the gold surfaces since it is related to the work function (W). In fact, measurements of E_{pzc} have been performed for thiol SAM covered Au(111) surfaces [47] revealing that they move in the negative direction as the hydrocarbon chain increases but they become more positive by introducing F atoms at the end of the hydrocarbon chain by changing the dipole moment. Considering that W is proportional to E_{pzc} [48] and that thiol adsorption markedly modifies the work function of clean metal surfaces [49] we have calculated W and ΔW values of all the thiols in their corresponding surface structures. The ΔW values follow the trend expected from equation [9] (Table 1). In fact, the magnitude of the perpendicular surface dipole ($\mu_\perp$) increases as the size of the non polarizable molecules increases, while its sign is determined by the relative polarizabilities of the head and tail groups of the molecules.

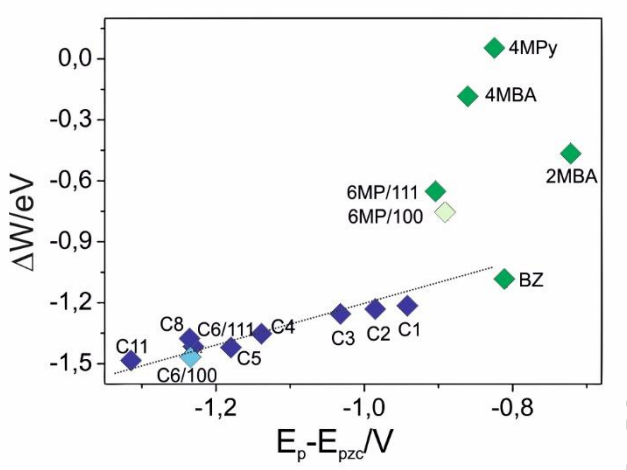

Figure 2. ΔW vs E_p-E_{pzc} *plot for the different thiol surface structures on Au(111) and Au(100)*

Figure 2 shows the ΔW vs (E_p–E_{pzc}) plot, which not only evaluates the energy involved in going from the thiol covered surface to the clean metal surface in the desorption process (ΔW), but also eliminates the contribution of the crystal face (E_p–E_{pzc}). First, we note that the use of (E_p–E_{pzc}) leads to a similar E_p value for the same SAM desorption (C6, 6MP) from Au(111) and Au(100) surfaces, revealing the role of the crystal face on E_p. Interestingly, results of our calculations show that a good linear correlation is obtained for alkanethiols with slope ≈ 1e, as expected for the reaction [1]. However, most of the aromatic thiols exhibit large changes in ΔW, due to the intrinsic molecular dipole moment [43] even for small (E_p-E_{pzc}) differences, i.e. E_p certainly does not reflect the changes in the work function for these thiols.

Now, we will consider the adsorption energy as a possible descriptor for the reductive desorption of the different thiols from the Au substrates.

Table 1

	Surface	RS	Unit Lattice	Θ	E_p/V	E_b*/eV	γ/meV. Å^{-2}	ΔW^*/eV
ALIPHATIC	Au(111)	C1	(3x4)	0.33	-0.71[50]	-2.41[34]	-107.3	-1,22
		C2	(3x4)	0.33	-0.75[51]	-2.61[52]	-116.4	-1.23
		C3	c(4x2)	0.33	-0.80[53]	-2.65[52]	-117.6	-1.26
		C4	c(4x2)	0.33	-0.91[6]	-2.76[34]	-122.8	-1.36
		C5	c(4x2)	0.33	-0.95[6]	-2.86[52]	-128.2	-1.44
		C6	c(4x2)	0.33	-1.0/1.07[6]	-2.98[34]	-132.1	-1.41
		C8	c(4x2)	0.33	-1.00[54]	-3.17[55]	-137.9	-1.37
		C11	c(4x2)	0.33	-1.08[16]	-3.52[16]	-157.1	-1.49
	Au(100)	C6	(2x7)	0.43	-1.14[56]	-3.05[57]	-151.0	-1.43
AROMATIC	Au(111)	4MBA	(√3x4)	0.25	-0.63[16]	-2.56[16]	-85.4	-0.18
		4MBA	c(4x2)	0.33	-0.63[16]	-2.49[16]	-111.0	-0.30
		2MBA	(√3x4)	0.12	-0.49[58]	-3.02[58]	-50.38	-0.47
		4MPy	(√3x5)	0.20	-0.59[59]	-2.10[59]	-56.2	0.06
		BZ	(√3x4)	0.25	-0.58[31]	-2.20[60]	-73.4	-1.11
HETERO CYCLIC	Au(111)	6MP	(3√3x2)	0.17	-0.67[61]	-2.93[60, 61]	-65.2	-0.67
	Au(100)	6MP	(3 × √10)	0.22	-0.81[62]	-3.24[62]	-83.0	-0.74
		6MP	(3√2 × √2)	0.33	-0.81[63]	-3.34[63]	-128.9	-0.77

#($\Delta W = W_{thiol} - W_{clean}$, $W_{cleanAu(111)} = 5.46$ eV $W_{cleanAu(100)} = 5.40$ eV)

Thus, we plot E_b^* vs (E_p-E_{pzc}) in Figure 3. There is a good correlation between aliphatic and some aromatic thiols (4MPy, BZ). However other aromatic and heterocyclic thiols exhibit more positive (E_p-E_{pzc}) (easier desorption) even when they have similar or larger E_b^* than the aliphatic thiols, i.e. no simple correlation is possible.

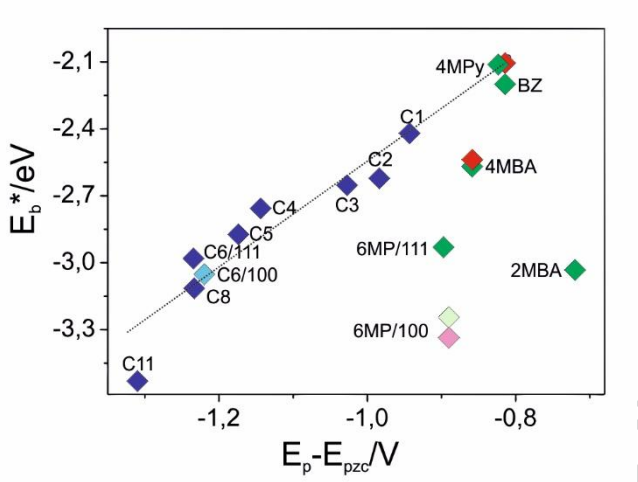

Figure 3. E_b* vs E_p-E_{pzc} plot. Blue symbols: alkanethiols on Au(111), light blue symbol: alkanethiol on Au(100), green symbols: aromatic/heterocyclic thiols, light green: heterocyclic thiols on Au(100). The red symbols correspond to denser surface structures for BZ and 4MBA and light red to 6MP in Au(100). The slope of the dashed line is 3e.

In order to understand this behavior we have calculated the molecule-Au interaction ($\Delta E_{m\text{-}Au}$), which includes the S-Au bond in most cases or additional O-Au or N-Au bonds present in some molecules, and the magnitude of the molecule-molecule interactions ($\Delta E_{m\text{-}m}$) for all thiols shown in Table 1. The results of our calculations (Table 2) reveal that $\Delta E_{m\text{-}Au}$ increases slightly with *n* for alkanethiols, and, more importantly, they are larger than those found in aromatic thiols (BZ, 4-MPy and 4-MBA). The exceptions are aromatic and heterocyclic molecules that have additional anchors to the Au substrate than the S atom, such as 2-MBA (additional O-Au bond) [58] and 6MP (additional N-Au bond) [30, 62]. These molecules have $\Delta E_{m\text{-}Au}$ values similar or higher than C11 (Table 2) although E_p is much more positive (Figure 3). On the other hand, the analysis of $\Delta E_{m\text{-}Au}$ also gives information about the stability of the different thiols in their SAMs. As expected, the DFT results for alkanethiols show that these interactions increase linearly with *n* with a slope 0.08 eV/C atom (Table 2), larger than the 0.03 eV/C atom experimentally found, due to the solvent contribution to the reaction [1]. On the other hand, molecules with simple π-π interactions such as the case of BZ have molecule-molecule interactions smaller than that found for alkanethiols of comparable size

such as C4-C6. This can be explained considering that typical distances between aromatic rings in these lattices are 0.4/0.5 nm, i.e. larger than the optimum π-π interaction distances (0.32/0.38 nm) [64] . However, this is not the case for aromatic thiols containing heteroatoms such as O or N where the magnitude of the vdW is larger than those estimated for alkanethiols. The presence of a heteroatom reduces the spatial extent of the π-electron cloud. Thus, a pyridine dimer binds more strongly than the benzene dimer in several configurations [65]. In conclusion, the E_b^* vs (E_p-E_{pzc}) cannot be used to rationalize the reductive desorption behavior of thiols. The aromatic (2-MBA, 4-MBA) and heterocyclic (6MP) thiols are the main missfitted data, since they have large E_b^*values, resulting from significant molecule-Au (double anchor) and molecule-molecule interactions, although they have an enhaced reductive desorption as shown in Figure 3. Also, the slope of the linear E_b^* vs (E_p-E_{pzc}) plot involving alkanethiols yields an unrealistic value of roughly 3 electrons per thiol, in contrast to the experimental evidence for the reaction [1].

Table 2

	ALIPHATIC								
Thiol	C_1	C_2	C_3	C_4	C_5	C_6	C_6/100	C_8	C_{11}
ΔE_{m-m} /eV	-0.07	-0.21	-0.23	-0.30	-0.38	-0.44	-0.42	-0.65	-0.95
ΔE_{m-Au} /eV	-2.34	-2.40	-2.42	-2.46	-2.48	-2.54	-2.63	-2.52	-2.57

	AROMATIC					HETEROCYCLIC		
Thiol	$4MBA_{0.25}$	$4MBA_{0.333}$	2MBA	4MPy	BZ	6MP	6MP/100	6MP/100
ΔE_{m-m} /eV	-0.56	-0.54	-0.11	-0.51	-0.18	-0.35	-0.33	-0.85
ΔE_{m-Au} /eV	-2.00	-1.95	-2.91	-1.59	-2.02	-2.58	-2.91	-2.49

Therefore, it is necessary to continue searching for a good correlation between theoretical and electrochemical data. In this sense, there are two experimental characteristics that are important to consider. First the aromatic thiols have smaller θ values than the aliphatic ones (Table 1), and it is known from STM data that they form more disordered SAMs [31]. On the other hand, it has been shown that the structural order of aromatic thiol SAMs on Au(111) can be considerably enhanced by increasing the number of phenyl rings in the molecular backbone [66-68] and by inserting the alkyl spacer between the phenyl ring and the sulfur

atom [69, 70]. Structural order in SAMs is a key point to improve their blocking ability for electron tranfer.[62, 71] Also, the introduction of methylene units leads to benzyl mercaptan to increase their coverage to 0.33 in relation to 0.25 observed for benzenethiol, thus resulting in better blocking ability [72]. Therefore, one can expect that E_p should depend not only on E_b^* but also on θ through the SAM order/disorder.

The Gibbs free energy of adsorption (γ) could end up being a better descriptor than E_b^* and W in the search for a correlation with E_p, since the desorption potential of a surfactant is the potential value at which the surface tension of the electrode/solvent becomes smaller than that of the electrode/surfactant (solvent) system. Note that γ captures both contributions, E_b^* and θ, (N_{RS}/A is proportional to θ) (equation [5]). Thus, in Figure 4 we have plotted γ vs (E_p- E_{pzc}) values for all thiols included in Table 1. A reasonable correlation is observed but with the thiols grouped into two families, aromatic/heterocyclic and aliphatic, which exhibit linear behavior with similar slopes but shifted by roughly 30 meV $Å^{-2}$, irrespective of the Au face. A key piece of information to understand this shift arises from 6MP and 4MBA SAMs on Au(100) and Au(111), respectively. A dense 6MP lattice (θ = 0.33) on Au(100) has been reported in addition to a diluted lattice with θ = 0.25 [30] (Table 1), both consisting of thiyls radicals. We observe that the γ value of the dense surface structure overlaps those of alkanethiols, which have the same coverage (red symbol in Figure 4), i.e. for the same coverage the difference in γ disappears. The formation of a dense 4MBA lattice with θ = 0.33 has also been reported, increasing immersion time/concentration in addition to the diluted lattice with θ = 0.25 [16]. In this case DFT calculations for a c(4x2) lattice similar to that of alkanethiols (i.e containing staples) leads to a γ value that also overlaps the linear plot corresponding to aliphatic thiols (red symbol in Figure 4). However, in this case, we have different adsorbed species: staples for the dense 4MBA phase and thiyl radicals for the diluted 4MBA lattice. In order to estimate the impact of the different adsorbed species in our

plots we have estimated the γ values of alkanethiols using adsorbed thiyl radicals rather than staples for the same surface coverage. Results (not shown in table 2) show that the γ values of alkanethiol SAM formed by thiyl radical staples still remain very close to the linear plot of alkanethiol SAMs consisting of staples. That is to say the presence of staples or thiyl radicals is not a key factor to explain the difference in γ values between aliphatic and aromatic/heteroclycic thiols. Finally, we have tested our conclusion by estimating the γ value for a hypothetical benzenethiol lattice formed by staples and θ = 0.33. Again the calculated γ (red symbol in Figure 4) overlaps the linear plot corresponding to alkanethiolates. Therefore, we can conclude that N_{RS}/A (θ) is the main parameter that controls the shift in the γ vs. E_p plot.

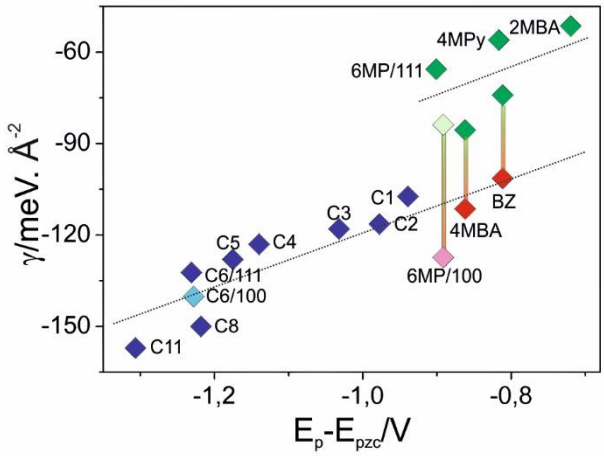

Figure 4. γ vs E_p-E_{pzc} plot. Blue symbols: alkanethiols on Au(111), light blue symbol: alkanethiol on Au(100), green symbols: aromatic/heterocyclic thiols, light green: heterocyclic thiols on Au(100). The red symbolds correspond to denser surface structures for 6MP, 4MBA and BZ while the solid lines indicate their shift from the upper linear plot.

The scatter in Figure 4 may have been due to the solubility of the desorbed products in the alkaline solution, repulsive effects in the SAM introduced by charged functional groups in solution or the different adsorption energies of the solvent on the crystal faces, considering that reaction [1] is a solvent substitution reaction. For instance, the E_p–E_{pzc} values for C6 and

6MP on the Au(111) and Au(100) faces are similar although the γ values indicate that they are more stable on the Au(100) face. This fact can be explained by considering the larger adsorption energy of water on the Au(100) (-0.3 eV) face [73] than on the Au(111) face (-0.15 eV) [74], which enhances thiol desorption and compensates the large adsorption energy of thiols on this face. Also, deviation in the reductive desorption of long alkanethiols, which takes place overlapping the hydrogen evolution reaction, is expected as the electrochemical reaction competes with the hydrogen induced desorption of thiols. [75, 76] Despite these limitations, in particular that the role of solvent is not included in our calculations, the data suggest that γ is the best parameter to describe the reductive behavior of thiols from the gold crystal surfaces.

ACKNOWLEDGMENTS

P.C. thankfully acknowledges MINECO (ENE2016-74899-C4-2-R, AEI-FEDER-UE) and the computer resources provided by the Computer Support Service for Research (SAII) at La Laguna University.

References

[1] Walczak MM, Popenoe DD, Deinhammer RS, Lamp BD, Chung CK, Porter MD. Reductive desorption of alkanethiolate monolayers at gold - a measure of surface coverage. Langmuir. 1991;7:2687-93.

[2] Yang DF, AlMaznai H, Morin M. Vibrational study of the fast reductive and the slow oxidative desorptions of a nonanethiol self-assembled monolayer from a Au(111) single crystal electrode. Journal of Physical Chemistry B. 1997;101:1158-66.

[3] Hobara D, Miyake O, Imabayashi S, Niki K, Kakiuchi T. In-situ scanning tunneling microscopy imaging of the reductive desorption process of alkanethiols on Au(111). Langmuir. 1998;14:3590-6.

[4] Vericat C, Vela ME, Benitez G, Carro P, Salvarezza RC. Self-assembled monolayers of thiols and dithiols on gold: new challenges for a well-known system. Chemical Society Reviews. 2010;39:1805-34.

[5] Zhong CJ, Porter MD. Fine structure in the voltammetric desorption curves of alkanethiolate monolayers chemisorbed at gold. Journal of Electroanalytical Chemistry. 1997;425:147-53.

[6] Widrig CA, Chung C, Porter MD. The electrochemical desorption of n-alkanethiol monolayers from polycrystalline Au and Ag electrodes. Journal of Electroanalytical Chemistry. 1991;310:335-59.

[7] Lee JW, Sim SJ, Cho SM, Lee J. Characterization of a self-assembled monolayer of thiol on a gold surface and the fabrication of a biosensor chip based on surface plasmon

resonance for detecting anti-GAD antibody. Biosensors & Bioelectronics. 2005;20:1422-7.
[8] Pissinis DE, Diaz C, Maza E, Bonini IC, Barrantes FJ, Salvarezza RC, et al. Functional nicotinic acetylcholine receptor reconstitution in Au(111)-supported thiolipid monolayers. Nanoscale. 2015;7:15789-97.
[9] Schilardi PL, Dip P, dos Santos Claro PC, Benítez GA, Fonticelli MH, Azzaroni O, et al. Electrochemical deposition onto self‐assembled monolayers: New insights into micro‐and nanofabrication. Chemistry‐A European Journal. 2006;12:38-49.
[10] Ponce I, Francisco Silva J, Onate R, Caroli Rezende M, Paez MA, Zagal JH, et al. Enhancement of the Catalytic Activity of Fe Phthalocyanine for the Reduction of O-2 Anchored to Au(111) via Conjugated Self-Assembled Mono layers of Aromatic Thiols As Compared to Cu Phthalocyanine. Journal of Physical Chemistry C. 2012;116:15329-41.
[11] O. Azzaroni MEV, G. Andreasen,P. Carro, and R. C. Salvarezza. Electrodesorption Potentials of Self-Assembled Alkanethiolate Monolayers on Ag(111) and Au(111). An Electrochemical, Scanning Tunneling Microscopy and Density Functional Theory Study. The Journal of Physical Chemistry B. 2002;106:12267–73.
[12] Sumi T, Uosaki K. Electrochemical oxidative formation and reductive desorption of a self-assembled monolayer of decanethiol on a Au(111) surface in KOH ethanol solution. Journal of Physical Chemistry B. 2004;108:6422-8.
[13] Kunze J, Leitch J, Schwan AL, Faragher RJ, Naumann R, Schiller S, et al. New method to measure packing densities of self-assembled thiolipid monolayers. Langmuir. 2006;22:5509-19.
[14] Laredo T, Leitch J, Chen M, Burgess IJ, Dutcher JR, Lipkowski J. Measurement of the charge number per adsorbed molecule and packing densities of self-assembled long-chain monolayers of thiols. Langmuir. 2007;23:6205-11.
[15] Seenath R, Leitch JJ, Su Z, Faragher RJ, Schwan AL, Lipkowski J. Measurements of surface concentration and charge number per adsorbed molecule for a thiolipid monolayer tethered to the Au(111) surface by a long hydrophilic chain. Journal of Electroanalytical Chemistry. 2017;793:203-8.
[16] González MCR, Orive AGl, Carro P, Salvarezza RC, Creus AHn. Structure and Electronic and Charge-Transfer Properties of Mercaptobenzoic Acid and Mercaptobenzoic Acid–Undecanethiol Mixed Monolayers on Au (111). The Journal of Physical Chemistry C. 2014;118:30013-22.
[17] Yang DF, Wilde CP, Morin M. Electrochemical desorption and adsorption of nonyl mercaptan at gold single crystal electrode surfaces. Langmuir. 1996;12:6570-7.
[18] Schilardi PL, Dip P, Claro PCD, Benitez GA, Fonticelli MH, Azzaroni O, et al. Electrochemical deposition onto self-assembled monolayers: New insights into micro-and nanofabrication. Chemistry-a European Journal. 2006;12:38-49.
[19] Vela ME, Martin H, Vericat C, Andreasen G, Creus AH, Salvarezza RC. Electrodesorption kinetics and molecular interactions in well-ordered thiol adlayers on Au(111). Journal of Physical Chemistry B. 2000;104:11878-82.
[20] Martin H, Vericat C, Andreasen G, Vela ME, Salvarezza RC. A Monte Carlo simulation for the stripping of the root 3x root 3 R30 degrees alkanethiol lattice from Au(111) terraces and steps. Journal of Chemical Physics. 2002;117:2293-8.
[21] Doneux T, Nichols RJ, Buess-Herman C. Dissolution kinetics of octadecanethiolate monolayers electro-adsorbed on Au(111). Journal of Electroanalytical Chemistry. 2008;621:267-76.
[22] Azzaroni O, Vela ME, Fonticelli M, Benitez G, Carro P, Blum B, et al. Electrodesorption potentials of self-assembled alkanethiolate monolayers on copper

electrodes. An experimental and theoretical study. Journal of Physical Chemistry B. 2003;107:13446-54.
[23] Grumelli D, Cristina LJ, Maza FL, Carro P, Ferron J, Kern K, et al. Thiol Adsorption on the Au(100)-hex and Au(100)-(1 X 1) Surfaces. Journal of Physical Chemistry C. 2015;119:14248-54.
[24] Zhong CJ, Zak J, Porter MD. Voltammetric reductive desorption characteristics of alkanethiolate monolayers at single crystal Au(111) and (110) electrode surfaces. Journal of Electroanalytical Chemistry. 1997;421:9-13.
[25] Arihara K, Ariga T, Takashima N, Arihara K, Okajima T, Kitamura F, et al. Multiple voltammetric waves for reductive desorption of cysteine and 4-mercaptobenzoic acid monolayers self-assembled on gold substrates. Physical Chemistry Chemical Physics. 2003;5:3758 - 61
[26] Munakata H, Oyamatsu D, Kuwabata S. Effects of omega-functional groups on pH-dependent reductive desorption of alkanethiol self-assembled monolayers. Langmuir. 2004;20:10123-8.
[27] Nuzzo RG, Dubois LH, Allara DL. Fundamental-studies of microscopic wetting on organic-surfaces .1. Formation and structural characterization of a self-consistent series of polyfunctional organic monolayers. Journal of the American Chemical Society. 1990;112:558-69.
[28] Lawrence H. Dubois BRZ, and Ralph G. Nuzzo. Molecular ordering of organosulfur compounds on Au(111) and Au(100): Adsorption from solution and in ultrahigh vacuum. The Journal of Chemical Physics. 1993;98:678.
[29] Peiretti LF, Quaino P, Tielens F. Competition between Two High-Density Assemblies of Poly(phenyl)thiols on Au(111). Journal of Physical Chemistry C. 2016;120:25462-72.
[30] Carro P, Müller K, Maza FL, Vericat C, Starke U, Kern K, et al. 6-Mercaptopurine Self-Assembled Monolayers on Gold (001)-hex: Revealing the Fate of Gold Adatoms. The Journal of Physical Chemistry C. 2017;121:8938-43.
[31] Kang H, Noh J. Influence of Thiol Molecular Backbone Structure on the Formation and Reductive Desorption of Self-Assembled Aromatic and Alicyclic Thiol Monolayers on Au(111) Surface. Bulletin of the Korean Chemical Society. 2013;34:1383-7.
[32] Vericat C, Vela ME, Corthey G, Pensa E, Cortés E, Fonticelli MH, et al. Self-assembled monolayers of thiolates on metals: a review article on sulfur-metal chemistry and surface structures. RSC Advances. 2014;4:27730-54.
[33] Hakkinen H. The gold-sulfur interface at the nanoscale. Nat Chem. 2012;4:443-55.
[34] Carro P, Pensa E, Vericat C, Salvarezza RC. Hydrocarbon Chain Length Induces Surface Structure Transitions in Alkanethiolate-Gold Adatom Self-Assembled Mono layers on Au(111). Journal of Physical Chemistry C. 2013;117:2160-5.
[35] Pensa E, Rubert A, Benitez G, Carro P, Orive AG, Creus AH, et al. Are 4-mercaptobenzoic acid self assembled monolayers on Au (111) a suitable system to test adatom models? The Journal of Physical Chemistry C. 2012;116:25765-71.
[36] Kresse G, Furthmuller J. Efficiency of ab-initio total energy calculations for metals and semiconductors using a plane-wave basis set. Computational Materials Science. 1996;6:15-50.
[37] Kresse G, Hafner J. Ab-initio molecular-dynamics for open-shell transition-metals. Physical Review B. 1993;48:13115-8.
[38] Dion M, Rydberg H, Schröder E, Langreth DC, Lundqvist BI. Van der Waals Density Functional for General Geometries. Physical Review Letters. 2004;92:246401.

[39] Klimes J, Bowler DR, Michaelides A. A critical assessment of theoretical methods for finding reaction pathways and transition states of surface processes. Journal of Physics: Condensed Matter 2010;22:074203-.
[40] Blöchl PE. Projector augmented-wave method. Physical Review B. 1994;50:17953-79.
[41] Monkhorst HJ, Pack JD. Special points for Brillouin-zone integrations. Physical Review B. 1976;13:5188-92.
[42] Pearson WB. Handbook of Lattice Spacing and Structure of Metals. New York: Pergamon Press, Inc.; 1958.
[43] Rusu PC, Brocks G. Work functions of self-assembled monolayers on metal surfaces by first-principles calculations. Physical Review B: Condensed Matter and Materials Physics. 2006;74:073414.
[44] Kolb DM, Schneider J. Surface reconstruction in electrochemistry: Au(100-(5 × 20), Au(111)-(1 × 23) and Au(110)-(1 × 2). Electrochimica Acta. 1986;31:929-36.
[45] Hromadova M, Fawcett WR. Studies of double-layer effects at single-crystal gold electrodes. 1. The reduction kinetics of hexaamminecobalt(III) ion in aqueous solutions. Journal of Physical Chemistry A. 2000;104:4356-63.
[46] Chen AC, Lipkowski J. Electrochemical and spectroscopic studies of hydroxide adsorption at the Au(111) electrode. Journal of Physical Chemistry B. 1999;103:682-91.
[47] Iwami Y, Hobara D, Yamamoto M, Kakiuchi T. Determination of the potential of zero charge of Au(111) electrodes modified with thiol self-assembled monolayers using a potential-controlled sessile drop method. Journal of Electroanalytical Chemistry. 2004;564:77-83.
[48] Conway BE, Bockris, John O'M., White, Ralph E. (Eds.) Modern Aspects of Electrochemistry. No 32. New York1999.
[49] Rusu PC, Brocks G. Surface dipoles and work functions of alkylthiolates and fluorinated alkylthiolates on Au(111). Journal of Physical Chemistry B. 2006;110:22628-34.
[50] Finklea HO. Electrochemistry of Organized Monolayers of Thiols and Related Molecules on Electrodes. New Jork: Marcel Dekker Inc.
[51] Imabayashi S, Iida M, Hobara D, Feng ZQ, Niki K, Kakiuchi T. Reductive desorption of carboxylic-acid-terminated alkanethiol monolayers from Au(111) surfaces. Journal of Electroanalytical Chemistry. 1997;428:33-8.
[52] Arce FT, Vela ME, Salvarezza RC, Arvia AJ. Complex structural dynamics at adsorbed alkanethiol layers at Au(111) single-crystal domains. Langmuir. 1998;14:7203-12.
[53] Zhang J, Chi Q, Ulstrup J. Assembly dynamics and detailed structure of 1-propanethiol monolayers on Au(111) surfaces observed real time by in situ STM. Langmuir. 2006;22:6203-13.
[54] Adamczyk LA. Understanding the Structure and Properties of
Self-Assembled Monolayers for Interfacial Patterning. Blacksburg: Virginiz; 2009.
[55] Carro P, Torrelles X, Salvarezza RC. A novel model for the ($\sqrt{3}\times\sqrt{3}$) R 30° alkanethiolate‐Au (111) phase based on alkanethiolate‐Au adatom complexes. Physical Chemistry Chemical Physics. 2014;16:19017-23.
[56] Grumelli D, Cristina LJ, Maza FL, Carro P, Ferrón J, Kern K, et al. Thiol Adsorption on the Au (100)-hex and Au (100)-(1× 1) Surfaces. The Journal of Physical Chemistry C. 2015;119:14248-54.
[57] Grumelli D, Maza FL, Kern K, Salvarezza RC, Carro P. Surface Structure and Chemistry of Alkanethiols on Au (100)-(1× 1) Substrates. The Journal of Physical Chemistry C. 2015;120:291-6.

[58] Rodríguez González MC, Carro P, Pensa E, Vericat C, Salvarezza R, Hernández Creus A. The Role of a Double Molecular Anchor on the Mobility and Self‐Assembly of Thiols on Au (111): the Case of Mercaptobenzoic Acid. ChemPhysChem. 2017.
[59] Ramirez EA, Cortes E, Rubert AA, Carro P, Benitez G, Vela ME, et al. Complex Surface Chemistry of 4-Mercaptopyridine Self-Assembled Monolayers on Au(111). Langmuir. 2012;28:6839-47.
[60] Carro P, Salvarezza RC. Unpublished Data. 2017.
[61] Pensa E, Carro P, Rubert AA, Benitez G, Vericat C, Salvarezza RC. Thiol with an Unusual Adsorption-Desorption Behavior: 6-Mercaptopurine on Au(111). Langmuir. 2010;26:17068-74.
[62] Maza FL, Grumelli D, Carro P, Vericat C, Kern K, Salvarezza RC. The role of the crystalline face in the ordering of 6-mercaptopurine self-assembled monolayers on gold. Nanoscale. 2016;8:17231-40.
[63] Carro P, Müller Kathrin, Lobo Maza, Flavia, Vericat, Carolina, Ulrich Starke, Klaus KErn, Roberto C Salvarezza and Doris Grumelli. 6-Mercaptopurine Self-Assembled Monolayers on Gold(001)-Hex:Revealing the Fate of Gold Adatoms. Journal of Physical Chemistry C2017. p. 6.
[64] Janiak C. A critical account on π–π stacking in metal complexes with aromatic nitrogen-containing ligands. J Chem Soc, Dalton Trans. 2000;0:3885-96
[65] Sherrill EGHaCD. Effects of Heteroatoms on Aromatic π−π Interactions: Benzene−Pyridine and Pyridine Dimer. The Journal of Physical Chemistry A. 2009;113:878-86.
[66] Dhirani AA, Zehner RW, Hsung RP, GuyotSionnest P, Sita LR. Self-assembly of conjugated molecular rods: A high-resolution STM study. Journal of the American Chemical Society. 1996;118:3319-20.
[67] Park JH, Noh JH, Han BS, Shin SS, Park IJ, Kim DH, et al. Influence of niobium doping in hierarchically organized titania nanostructure on performance of dye-sensitized solar cells. Journal of Nanoscience and Nanotechnology. 2012;12:5091-5.
[68] Bashir A, Azzam W, Rohwerder M, Terfort A. Polymorphism in Self-Assembled Terphenylthiolate Monolayers on Au(111). Langmuir. 2013;29:13449-56.
[69] Noh J, Ito E, Hara M. Self-assembled monolayers of benzenethiol and benzenemethanethiol on Au(111): Influence of an alkyl spacer on the structure and thermal desorption behavior. Journal of Colloid and Interface Science. 2010;342:513-7.
[70] Kang H, Lee S, Ito E, Hara M, Noh J. An Alkyl Spacer Effect on the Structure of 4-Fluorobenzenethiol and 4-Fluorobenzenemethanethiol Self-Assembled Monolayers on Au(111). Journal of Nanoscience and Nanotechnology. 2012;12:4274-8.
[71] Noh J. Formation and structure of cyclopentanethiol self-assembled monolayers on Au(111). Bulletin of the Korean Chemical Society. 2006;27:944-6.
[72] Fonticelli M, Azzaroni O, Benitez G, Martins M, Carro P, Salvarezza R. Molecular Self-Assembly on Ultrathin Metallic Surfaces: Alkanethiolate Monolayers on Ag (1× 1)− Au (111). The Journal of Physical Chemistry B. 2004;108:1898-905.
[73] Grob XLaA. First-principles study of the water structure on flat and stepped gold surfaces. Surface Science. 2012;601:886-91.
[74] Ahmed Huzayyin JHC, Keryn Lian, and Francis Dawson. Interaction of Water Molecule with Au(111) and Au(110) Surfaces
under the Influence of an External Electric Field. The Journal of Physial chemistry C. 2014;118:3459-70.
[75] Kautz NA, Kandel SA. Alkanethiol/Au(111) Self-Assembled Monolayers Contain Gold Adatoms: Scanning Tunneling Microscopy before and after Reaction with Atomic Hydrogen. Journal of the American Chemical Society. 2008;130:6908-9.

[76] Pensa E, Vericat C, Grumelli D, Salvarezza RC, Park SH, Longo GS, et al. New insight into the electrochemical desorption of alkanethiol SAMs on gold. Physical Chemistry Chemical Physics. 2012;14:12355-67.

Graphical Abstract